

Electronic Supplementary Information (ESI)

Effect of Chirality on the Optical Properties of Layered Hybrid Perovskite R- and S- α -Methylbenzylammonium Lead Iodide

Tariq Sheikh, Shabnum Maqbool, Parikshit Kumar Rajput, Pankaj Mandal and Angshuman Nag*

Department of Chemistry, Indian Institute of Science Education and Research (IISER) Pune,
411008 (India)

*Email: angshuman@iiserpune.ac.in

Experimental Section

Chemicals

Lead(II) oxide (Sigma Aldrich, 99.9%), hydriodic acid (Sigma Aldrich, 57% w/w in H₂O, 99.9%), hypophosphorous acid (Avra, 50% w/w H₂O), R-(+)- α -methylbenzylamine (Sigma Aldrich, 99%), S-(-)- α -methylbenzylamine (Sigma Aldrich, 99%), racemic- α -methylbenzylamine (Sigma Aldrich, 98%), acetonitrile (Sigma Aldrich, 99.8%), diethyl ether (Rankem, 99.5%).

Synthesis of (Rac-, R- and S- α -MBA)₂PbI₄ single crystals

(Rac-, R- or S- α -MBA)₂PbI₄ single crystals were synthesized by three separate reactions using an aqueous acid precipitation method.¹ For example, to prepare (Rac- α -MBA)₂PbI₄, 2.5 mmol (558 mg) lead(II) oxide was dissolved in a mixture of 10 mL aqueous hydriodic acid (57% w/w in H₂O) and 2 mL aqueous hypophosphorous acid (50% w/w H₂O) by heating to boiling under constant magnetic stirring. Once clear yellow solution was obtained, 5 mmol of racemic- α -methylbenzylamine was added to the vial. The stirring was stopped once a clear yellow solution was obtained. The solution was allowed to cool down to room temperature naturally. During the cooling process, orange-colored crystals of (Rac- α -MBA)₂PbI₄ started to crystalize. The crystals were filtered and washed with diethyl ether and dried under vacuum.

For the synthesis of (R- α -MBA)₂PbI₄ single crystals, exactly same procedure was followed with only difference being the use of R-(+)- α -methylbenzylamine as the organic amine in place of racemic- α -methylbenzylamine. Similarly, the (S- α -MBA)₂PbI₄ single crystals were synthesized by using S-(-)- α -methylbenzylamine as the organic amine.

Preparation of (Rac-, R- and S- α -MBA)₂PbI₄ thin films

(Rac-, R- or S- α -MBA)₂PbI₄ thin films were prepared on sapphire substrates. First, the sapphire substrates were washed with water, followed by isopropanol and finally by acetone. 10 mg each of (Rac-, R- or S- α -MBA)₂PbI₄ single crystals were separately dissolved in 0.5 mL acetonitrile. These solutions were then spin-coated on the freshly cleaned sapphire substrates at the spinning rate of 3000 rpm for 20 s. The sapphire substrates were pre-heated at 70 °C before spin coating.

Characterization

Single crystal X-ray diffraction (XRD) data were collected on Bruker Smart Apex Duo diffractometer at 100 K using Mo K α radiation ($\lambda = 0.71073 \text{ \AA}$). The frames were integrated with the Bruker SAINT software package by a narrow-frame algorithm. The structures were solved by a direct method and refined by full-matrix least-squares on F^2 using the SHELXTL software package. The PbX₄ framework was refined anisotropically without any constraint. The organic atoms were also refined anisotropically but with constraints on the C-C and C-N bond lengths. Powder XRD measurements were carried on Bruker D8 Advance X-ray diffractometer using Cu K α radiation (1.54 \AA). UV-Visible absorbance data were measured on Cary Series UV-Vis Spectrophotometer (Agilent Technologies). The absorbance spectra were recorded in transmittance mode. Circular dichroism (CD) measurements were carried at room temperature on a Jasco J-815 spectropolarimeter. The CD spectra were measured at a scan speed of 50 nm per minute with 0.5 nm resolution and response time of 1 s. The CD spectra were also recorded in transmittance mode.

The room temperature steady-state photoluminescence (PL) measurements were carried on FLS 980 (Edinburgh Instruments). The samples were excited with a 405 nm laser. The temperature-dependent steady-state PL measurements were carried on the same instrument. For the temperature-dependent PL measurements, films of samples on sapphire substrates were mounted on a gold-plated sample holder. The sample holder was then mounted on the cold finger attached to a closed-cycle helium cryostat (Advanced Research Systems). The cryostat was connected to a temperature controller (Lake Shore Cryotronics) to achieve the desired temperatures.

Nonlinear Optics: The non-linear optical measurements were carried on a home-built setup.² The excitation wavelengths for the second and third harmonic generation (SHG/THG) are obtained from optical parametric amplifier (OPA, Light Conversion) which generates radiation between 250-2600 nm. The OPA is pumped by ultrafast 45 fs pump pulses centered around 800 nm obtained from the regenerative amplifier (Spitfire Pro, Spectra physics) seeded by an ultrafast oscillator (Tsunami, Spectra Physics). The excitation pulses from OPA are filtered by an 850 nm long pass filter to allow only near- IR wavelengths to excite the sample and block the visible stray radiation from the OPA. These pulses are focused by a 200 mm plano-convex lens on to the sample (sandwiched between two quartz slides) placed ahead of the focal point. An attenuator is employed

to modulate the excitation wavelength intensity. The generated SHG/THG obtained from the sample is collimated using a 25 mm plano-convex lens into an optical fiber which is coupled to the spectrometer. For the polarization dependent measurements, an assembly of Glan Polarizer and half-wave plate is utilized to modulate the polarization of the incident light. The sample is mounted on a rotational mount to vary the crystal orientation with respect to incident light polarization direction.

Table S1: Crystal structure and data refinement of (Rac-, R- and S- α -MBA)₂PbI₄ at 296 K.

	(R- α -MBA) ₂ PbI ₄	(S- α -MBA) ₂ PbI ₄	(Rac- α -MBA) ₂ PbI ₄
CCDC Numbers	2162948	2162950	2162947
Chemical formula	C ₁₆ H ₂₄ I ₄ N ₂ Pb	C ₁₆ H ₂₄ I ₄ N ₂ Pb	C ₁₆ H ₂₄ I ₄ N ₂ Pb
Formula weight	959.16 g/mol	959.16 g/mol	959.16 g/mol
Temperature	296(2) K	296(2) K	296(2) K
Wavelength	0.71073 Å	0.71073 Å	0.71073 Å
Crystal system	Orthorhombic	Orthorhombic	Monoclinic
Space group	<i>P</i> 2 ₁ 2 ₁ 2 ₁	<i>P</i> 2 ₁ 2 ₁ 2 ₁	<i>P</i> 2 ₁ / <i>c</i>
Unit cell dimensions	a = 8.8203(10) Å b = 9.1821(10) Å c = 28.579(3) Å $\alpha = \beta = \gamma = 90^\circ$	a = 8.8315(13) Å b = 9.1847(13) Å c = 28.569(4) Å $\alpha = \beta = \gamma = 90^\circ$	a = 14.660(3) Å b = 9.3799(19) Å c = 8.7777(18) Å $\alpha = \gamma = 90^\circ, \beta = 100^\circ$
Volume	2314.6(5) Å ³	2317.4(6) Å ³	1189.2(4) Å ³
Z	4	4	2
Density	2.753 g/cm ³	2.749 g/cm ³	2.679 g/cm ³
Abs. coefficient	12.626 mm ⁻¹	12.611 mm ⁻¹	12.288 mm ⁻¹
Theta range	2.33 to 28.29°	3.50 to 26.37°	2.59 to 25.34°
Index ranges	-11 ≤ h ≤ 11, -10 ≤ k ≤ 12, -38 ≤ l ≤ 38	-11 ≤ h ≤ 10, -11 ≤ k ≤ 11, -35 ≤ l ≤ 35	-19 ≤ h ≤ 19, -12 ≤ k ≤ 12, -11 ≤ l ≤ 9
Reflections collected	41748	27087	19867
Independent reflections	5682 [R(int) = 0.0635]	4706 [R(int) = 0.0708]	2128 [R(int) = 0.0433]
Coverage	99.80%	99.6%	97.7%
Absorption correction	Multi-Scan	Multi-scan	Multi-scan
Structure solution	Direct methods	Direct method	Direct method
Structure solution program	SHELXT 2014/5 (Sheldrick, 2014)	SHELXT 2014/5 (Sheldrick, 2014)	SHELXT 2014/5 (Sheldrick, 2014)
Refinement method	Full-matrix least-squares on F ²	Full-matrix least-squares on F ²	Full-matrix least-squares on F ²
Refinement program	SHELXL-2018/3 (Sheldrick, 2018)	SHELXL-2018/3 (Sheldrick, 2018)	SHELXL-2018/3 (Sheldrick, 2018)
Function minimized	$\Sigma w(F_o^2 - F_c^2)^2$	$\Sigma w(F_o^2 - F_c^2)^2$	$\Sigma w(F_o^2 - F_c^2)^2$
Data / parameters	5682 / 173	4706 / 173	2128 / 98
Goodness-of-fit on F ²	0.995	0.737	1.373
Final R indices; I>2 σ (I)	R1 = 0.0838, wR2 = 0.1785	R1 = 0.0761, wR2 = 0.1696	R1 = 0.0764, wR2 = 0.1575
all data	R1 = 0.0902, wR2 = 0.1833	R1 = 0.0840, wR2 = 0.1758	R1 = 0.1089, wR2 = 0.1700
Weighting scheme	w=1/[$\sigma^2(F_o^2)+(0.02000P)^2 + 8.000P$] P=(F _o ² +2F _c ²)/3	w=1/[$\sigma^2(F_o^2)+(0.0500P)^2 + 10.5000P$] P=(F _o ² +2F _c ²)/3	w=1/[$\sigma^2(F_o^2)+(0.1000P)^2 + 10.0000P$] P=(F _o ² +2F _c ²)/3
Largest diff. peak, hole	2.005, -0.531 eÅ ⁻³	1.176, -0.606 eÅ ⁻³	0.850, -0.800 eÅ ⁻³
R.M.S. deviation	0.092 eÅ ⁻³	0.064 eÅ ⁻³	0.159 eÅ ⁻³

Table S2: Crystal structure and data refinement of (Rac-, R- and S- α -MBA)₂PbI₄ at 100 K.

	(R- α -MBA) ₂ PbI ₄	(S- α -MBA) ₂ PbI ₄	(Rac- α -MBA) ₂ PbI ₄
CCDC Numbers	2175511	2175510	2175509
Chemical formula	C ₁₆ H ₂₄ I ₄ N ₂ Pb	C ₁₆ H ₂₄ I ₄ N ₂ Pb	C ₁₆ H ₂₄ I ₄ N ₂ Pb
Formula weight	959.16 g/mol	959.16 g/mol	959.16 g/mol
Temperature	100(2) K	100(2) K	100(2) K
Wavelength	0.71073 Å	0.71073 Å	0.71073 Å
Crystal system	Orthorhombic	Orthorhombic	Monoclinic
Space group	<i>P</i> 2 ₁ 2 ₁ 2 ₁	<i>P</i> 2 ₁ 2 ₁ 2 ₁	<i>P</i> 2 ₁ / <i>c</i>
Unit cell dimensions	a = 8.853(2) Å b = 9.220(2) Å c = 28.642(8) Å $\alpha = \beta = \gamma = 90^\circ$	a = 8.846(3) Å b = 9.196(3) Å c = 28.620 (10) Å $\alpha = \beta = \gamma = 90^\circ$	a = 14.458(3) Å b = 9.2720(19) Å c = 8.7055(17) Å A = $\gamma = 90^\circ$, $\beta = 100^\circ$
Volume	2337.9(10) Å ³	2328.2(14) Å ³	1149.5(4) Å ³
Z	4	4	2
Density	2.725 g/cm ³	2.736 g/cm ³	2.771 g/cm ³
Abs. coefficient	12.500 mm ⁻¹	12.552 mm ⁻¹	12.711 mm ⁻¹
Theta range	5.11 to 25.35°	2.33 to 28.31°	2.62 to 25.35°
Index ranges	-10 ≤ h ≤ 10, -10 ≤ k ≤ 11, -34 ≤ l ≤ 34	-11 ≤ h ≤ 11, -12 ≤ k ≤ 12, -38 ≤ l ≤ 38	-19 ≤ h ≤ 19, -10 ≤ k ≤ 12, -10 ≤ l ≤ 11
Reflections collected	46054	42153	19674
Independent reflections	4176 [R(int) = 0.0928]	5764 [R(int) = 0.0761]	2105 [R(int) = 0.0404]
Coverage	97.2%	99.6%	99.6%
Absorption correction	Multi-Scan	Multi-scan	Multi-scan
Structure solution	Direct methods	Direct method	Direct method
Structure solution program	SHELXT 2014/5 (Sheldrick, 2014)	SHELXT 2014/5 (Sheldrick, 2014)	SHELXT 2014/5 (Sheldrick, 2014)
Refinement method	Full-matrix least-squares on F ²	Full-matrix least-squares on F ²	Full-matrix least-squares on F ²
Refinement program	SHELXL-2018/3 (Sheldrick, 2018)	SHELXL-2018/3 (Sheldrick, 2018)	SHELXL-2018/3 (Sheldrick, 2018)
Function minimized	$\Sigma w(F_o^2 - F_c^2)^2$	$\Sigma w(F_o^2 - F_c^2)^2$	$\Sigma w(F_o^2 - F_c^2)^2$
Data / parameters	4176 / 173	4764/ 173	2105 / 110
Goodness-of-fit on F ²	0.603	1.029	1.293
Final R indices; I>2 σ (I)	R1 = 0.0648, wR2 = 0.1631	R1 = 0.0722, wR2 = 0.1684	R1 = 0.00623, wR2 = 0.1317
all data	R1 = 0.0725, wR2 = 0.1693	R1 = 0.0773, wR2 = 0.1719	R1 = 0.0754, wR2 = 0.1438
Weighting scheme	w=1/[$\sigma^2(F_o^2)+(0.10000P)^2 + 0.0400P$] P=(F _o ² +2F _c ²)/3	w=1/[$\sigma^2(F_o^2)+(0.0500P)^2 + 1.0000P$] P=(F _o ² +2F _c ²)/3	w=1/[$\sigma^2(F_o^2)+(0.0100P)^2 + 2.5000P$] P=(F _o ² +2F _c ²)/3
Largest diff. peak, hole	0.053, -0.024 eÅ ⁻³	0.892, -0.255 eÅ ⁻³	0.530, -0.413 eÅ ⁻³
R.M.S. deviation	0.003 eÅ ⁻³	0.036 eÅ ⁻³	0.075 eÅ ⁻³

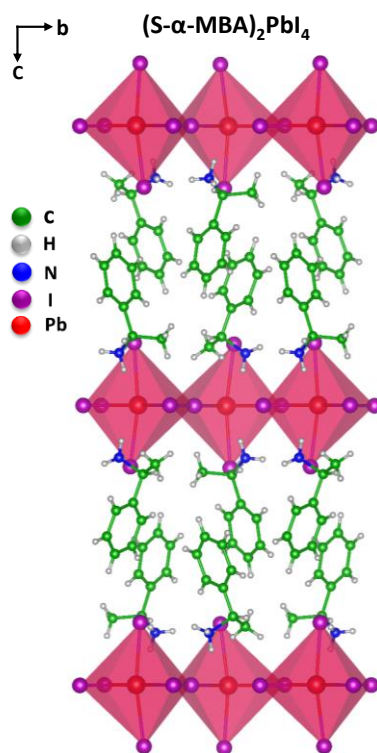


Figure S1: Crystal structures of $(S\text{-}\alpha\text{-MBA})_2\text{PbI}_4$ obtained by solving the single crystal XRD data recorded at RT (296 K).

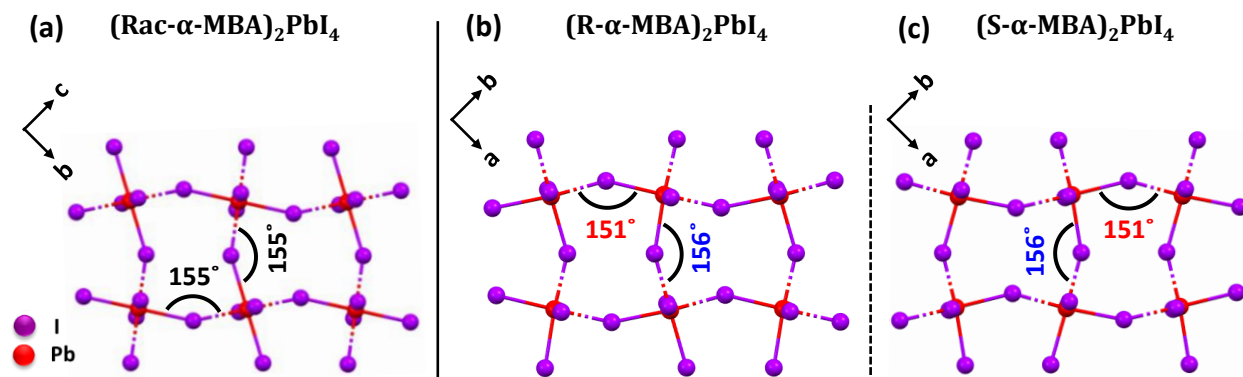


Figure S2: Top view of the 2D Pb-I layers in (a) $(\text{Rac-}\alpha\text{-MBA})_2\text{PbI}_4$, (b) $(\text{R-}\alpha\text{-MBA})_2\text{PbI}_4$, and (c) $(\text{S-}\alpha\text{-MBA})_2\text{PbI}_4$ showing Pb-I-Pb bond angles. Two types of Pb-I-Pb bond angles are present in the chiral (R- and S- α -MBA) $_2$ PbI $_4$, whereas a single type of Pb-I-Pb bond angle is observed in $(\text{Rac-}\alpha\text{-MBA})_2\text{PbI}_4$. Figures a-c are obtained by solving the single crystal XRD data recorded at RT (296 K).

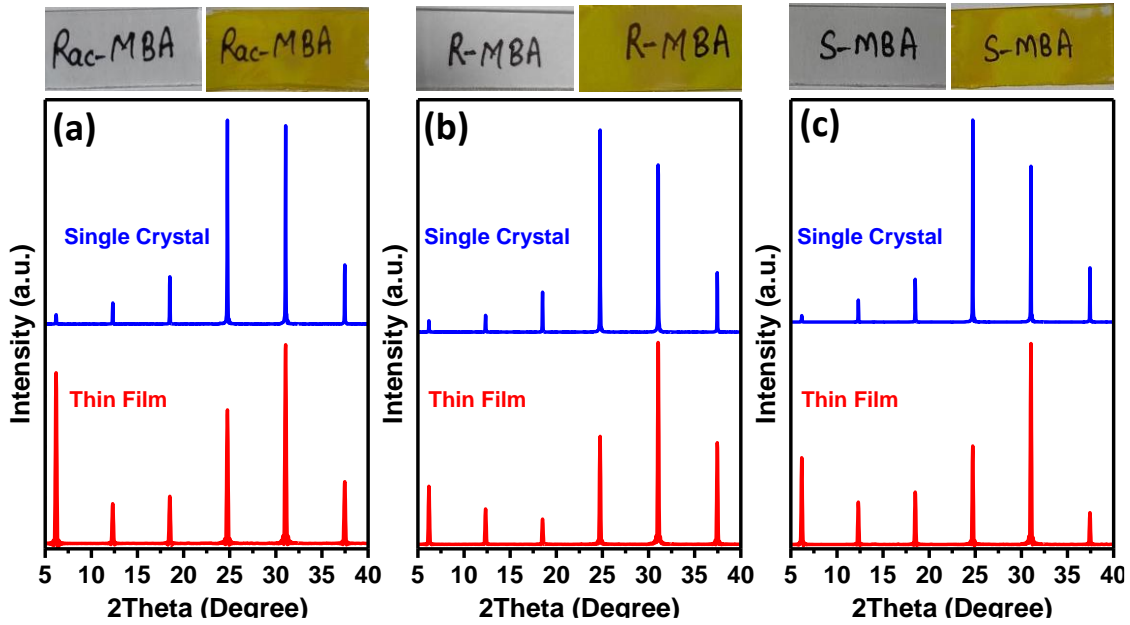


Figure S3: Powder XRD patterns of as-prepared (a) Rac-, (b) R- and (c) S- (α -MBA) $_2$ PbI $_4$ thin films overlapped with that of the (Rac-, R- and S- α -MBA) $_2$ PbI $_4$ single crystals. Top panel shows the optical photographs of the blank glass substrates and the as-prepared (Rac-, R- and S- α -MBA) $_2$ PbI $_4$ thin films (yellow color).

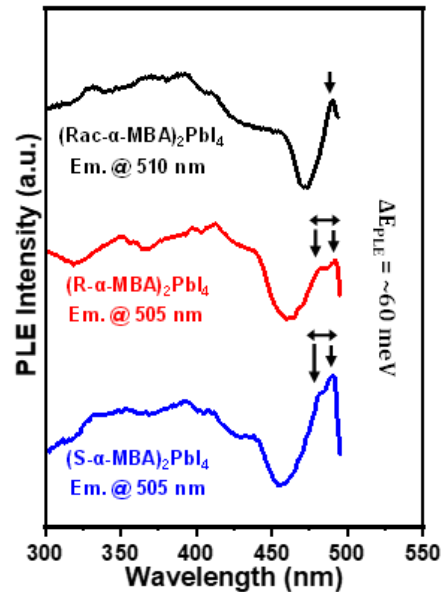


Figure S4: PL excitation (PLE) spectra of (Rac-, R- and S- α -MBA) $_2$ PbI $_4$, recorded at 5 K. The spectra are normalized from 0 to 1, and then shifted vertically for clarity of presentation. ΔE_{PLE} is the energy difference between the two peaks observed in the excitonic region of the (R- and S- α -MBA) $_2$ PbI $_4$.

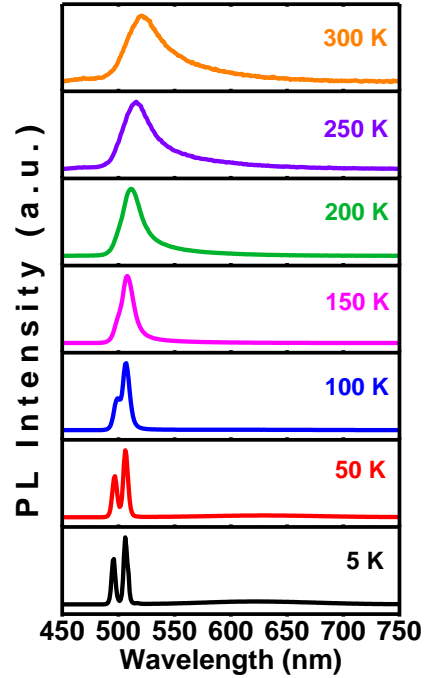


Figure S5: Temperature-dependent PL spectra of $(S\text{-}\alpha\text{-MBA})_2\text{PbI}_4$ thin film.

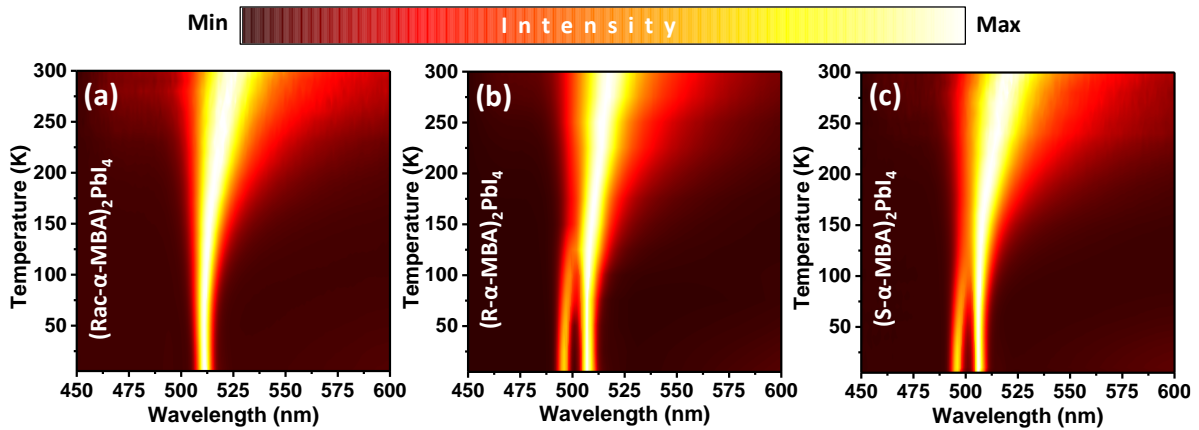


Figure S6: Pseudocolor maps of temperature-dependent PL spectra of (a) $(\text{Rac-}\alpha\text{-MBA})_2\text{PbI}_4$, (b) $(\text{R-}\alpha\text{-MBA})_2\text{PbI}_4$, and (c) $(\text{S-}\alpha\text{-MBA})_2\text{PbI}_4$ thin films. The PL intensities in all the spectra are normalized from 0 to 1.

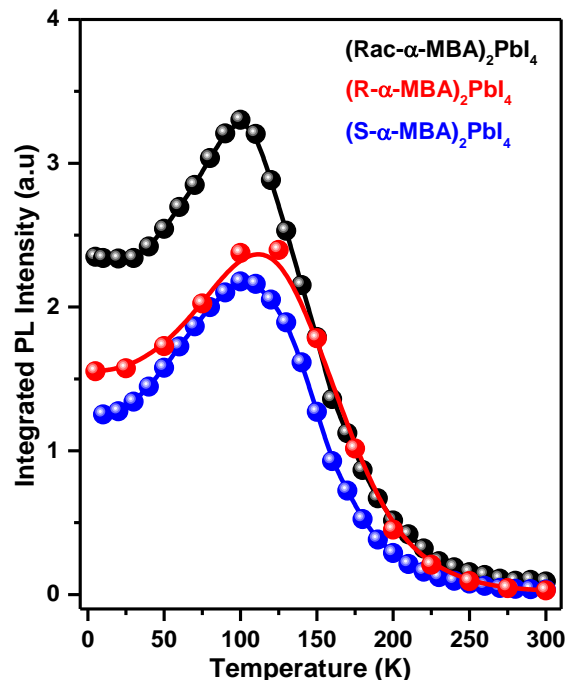


Figure S7: Variation of the integrated PL intensity with temperature for (Rac-, R- and S- α -MBA) $_2$ PbI $_4$. For (R- and S- α -MBA) $_2$ PbI $_4$, integration is done over both the PL peaks. The colored symbols represent the experimental data, and the lines are just guides to the eye.

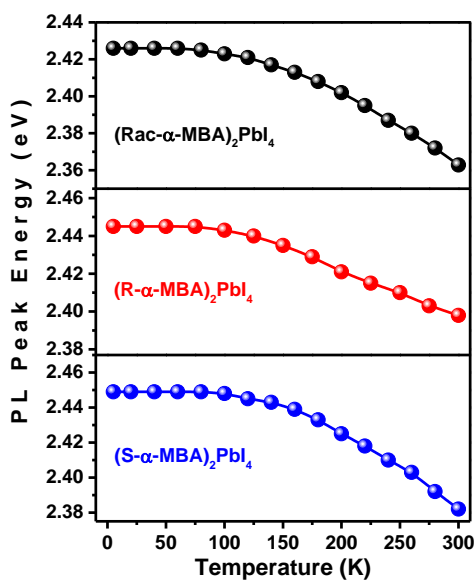


Figure S8: Variation of the PL peak energy of the main peak (longer-wavelength or lower-energy peak for the samples that show two peaks) with temperature for (Rac-, R- and S- α -MBA) $_2$ PbI $_4$. The colored symbols represent the experimental data, and the lines are just a guides to the eye.

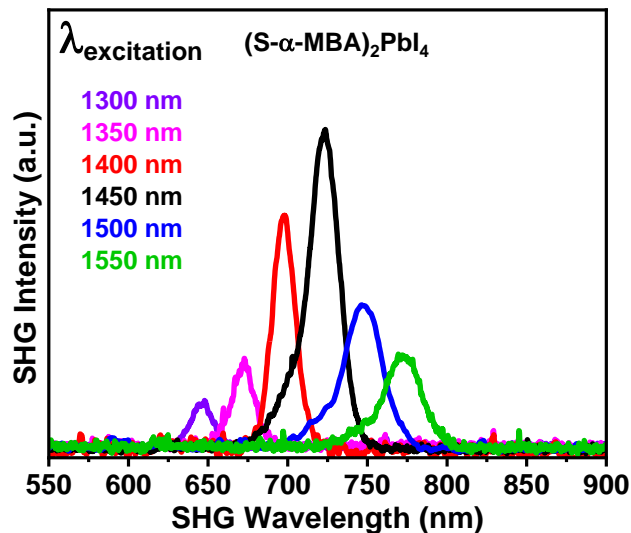


Figure S9: SHG spectra of $(S-\alpha\text{-MBA})_2\text{PbI}_4$. The samples were excited in 1300 to 1600 nm wavelength range at a constant power of 5 mW.

Polarization dependence of second harmonic generation: For the polarization-dependent SHG measurements, the (R- and S- α -MBA) $_2$ PbI $_4$ crystals were loaded in a rotating sample mount. The crystals were oriented in such a way that the a-axis of the crystal is parallel to the vertically polarized light. The a-axes of the crystals were determined by the face indexing using single crystal XRD as shown in Figure S10. The direction of polarization of the incident light was modulated by a half-wave plate. Incident light having polarizations along different directions was focused on the crystal, and SHG output was recorded. The SHG output showed a strong dependence on the direction of polarization of incident light. The angle between the a-axis of the crystal and the direction of polarization of incident light is represented by “ θ ”. Figure S11 shows the vertically ($\theta = 0^\circ$) and horizontally ($\theta = 90^\circ$) polarized light with respect to the a-axis of the crystal. In both (R- and S- α -MBA) $_2$ PbI $_4$ crystals, almost no SHG response was obtained when the direction of polarization was vertical (i.e., $\theta = 0^\circ$). As the θ increased, the intensity of SHG increased. The intensity of the SHG signal reached the maximum when the θ reached 90° . With further increase in θ , the SHG output reversed its trend and reached to zero at $\theta = 180^\circ$. Upon rotating the direction of polarization by 360° , a bi-lobed SHG behavior was observed as shown in Figure 3b of main manuscript and Figure S12 of ESI. This two-lobed behavior suggests that the SHG in both (R- and S- α -MBA) $_2$ PbI $_4$ crystals show an anisotropic behavior.

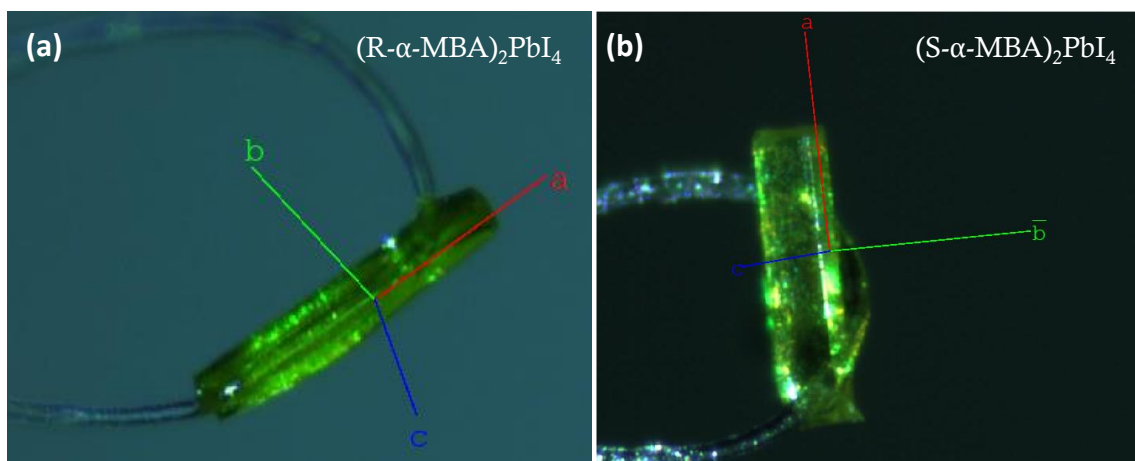


Figure S10: Photograph of (a) $(R-\alpha\text{-MBA})_2\text{PbI}_4$ and (b) $(R-\alpha\text{-MBA})_2\text{PbI}_4$ single crystals, on the goniometer head, under the X-rays, showing the crystallographic axes in the crystal.

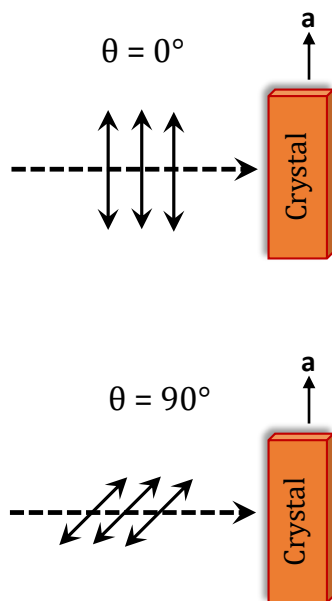


Figure S11: Schematics showing the direction of polarization of incident light with respect to the a-axis of the crystal.

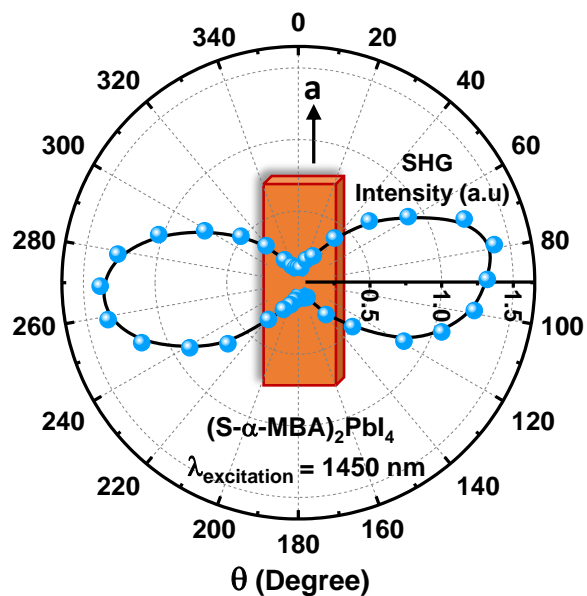


Figure S12: Variation of SHG intensity in $(S-\alpha\text{-MBA})_2\text{PbI}_4$ with the change in the direction of polarization of incident light. θ is the angle between the a-axis of the crystal and the direction of polarization of incident light. Orange Cuboid represents the $(S-\alpha\text{-MBA})_2\text{PbI}_4$ crystal. The blue spheres represent the experimental data and the black line is guide to the eye.

References

1. D. G. Billing and A. Lemmerer, *CrystEngComm*, 2006, **8**, 686-695.
2. S. Maqbool, T. Sheikh, Z. Thekkayil, S. Deswal, R. Boomishankar, A. Nag and P. Mandal, *J. Phys. Chem. C*, 2021, **125**, 22674-22683.